Pure and Binary Adsorption Equilibria of Carbon Dioxide and Nitrogen on Silicalite

Peiyuan Li and F. Handan Tezel*

Department of Chemical and Biological Engineering, Faculty of Engineering, University of Ottawa, 161 Louis Pasteur, Ottawa, Ontario K1N 6N5, Canada

For different separation applications of CO_2 and N_2, pure and mixture adsorption isotherms of these gases on silicalite adsorbent were determined experimentally. Constant volume and concentration pulse chromatographic techniques were used for the determination of pure and binary adsorption behavior, respectively. Pure component isotherms were determined up to 5 bar pressure for the temperature range (40 to 100) °C. Binary adsorption behavior for CO_2 and N_2 mixtures, covering the whole concentration range, were determined experimentally for a total pressure of 1 bar for the same temperature range. The applicability of different pure adsorption isotherm models was discussed for the pure isotherms, and ideal separation factors were determined. For the mixture adsorption isotherms, three binary concentration pulse methods, HT−CPM (Harlick and Tezel−Concentration Pulse Method), MTT−CPM (Modified Triebe and Tezel−Concentration Pulse Method), and MVV−CPM (Modified Van der Vlist and Van der Meijden−Concentration Pulse Method) were considered, and HT−CPM was found to be the most applicable one for this particular system. The experimental binary isotherms were compared to the predicted ones by using different binary adsorption models for this system. The results obtained showed that silicalite is a promising adsorbent for the separation of CO_2 and N_2.

Introduction

The global environment is a major issue today, and global warming in particular is the focus of much attention. Accumulation of greenhouse gases (GHG) in the atmosphere is responsible for increased global warming of our planet. It is supposed that the increasing concentration of carbon dioxide mainly from flue gas and automobile emissions into the atmosphere is the major contributor to this problem.[1,2] A variety of techniques have been studied for CO_2-N_2 adsorption separation in the literature.[3–22]

Silicalite is widely used as a selective adsorbent. Its intermediate (ten-ring) pore size leads to molecular sieve size selectivity. It has high thermal and hydrothermal stability. Its Si/Al ratio is in the thousands, so it has hydrophobic and organophilic adsorptive properties.[23]

The volumetric method involves measuring the pressure change in a known volume of gas subjected to an adsorbent sample. As the gas is adsorbed and allowed to come to equilibrium, the measured decrease in the closed system pressure yields the amount of gas adsorbed under the given conditions. This static method has been used extensively to determine adsorption isotherms.[24,25]

One dynamic method of analysis for adsorption systems is the use of the concentration pulse chromatographic technique. In the literature, methods using the K_p-functions for determining binary adsorption isotherms from concentration pulse chromatographic data have been given and shown capable of interpreting highly selective binary systems.[9,26–31]

In this current work, adsorption separation of carbon dioxide and nitrogen on silicalite was studied. Pure and binary adsorption isotherms were obtained by the constant volume and the concentration pulse chromatographic techniques, respectively. The thermodynamic consistency tests between pure and binary gas adsorption systems were also discussed.

* Corresponding author. E-mail: handan.tezel@uottawa.ca. Tel.: 613-562-5800. Ext. 6099. Fax: 613-562-5172.

Methods

There are many approaches for fitting adsorption isotherms for pure gas systems. Among two-parameter models, the simplest and still the most useful pure gas isotherm is the Langmuir isotherm.[32,33] The Freundlich isotherm is another two-parameter model that is commonly used.[34]

Three-parameter adsorption isotherm models are more flexible. For example, the Sips (Langmuir−Freundlich) isotherm[35] is superior for data correlation covering wide ranges of pressures and temperatures when both Langmuir and Freundlich isotherms fail.[25] Other three-parameter isotherms that are popular, and satisfy both low and high ends of the pressure range, are the Toth and multisite Langmuir isotherms.[33] Employing the Flory−Huggins form of activity coefficient for adsorption, vacancy solution theory is another three-parameter isotherm which was first developed in 1980.[33,36,37] The dual-site−Langmuir (DSL) model, a four-parameter isotherm, distinguishes two categories of different active sorption sites in the adsorbent, each one following a Langmuir adsorption behavior.[38]

The temperature dependence of equilibrium parameters is required for the purpose of extrapolation or interpolation of equilibrium data to other temperatures as well as the calculation of the isosteric heat of adsorption. The temperature dependence of the Sips and Toth equations for the affinity constants B may take the following form

$$B = B_0 e^{\frac{Q}{RT_0}\left(\frac{T_0}{T}-1\right)} \quad (1)$$

where B_0 is the adsorption affinity constant at some reference temperature T_0; Q is the isosteric heat, invariant with the surface

10.1021/je700183y CCC: $40.75
Published on Web 09/25/2008

Table 1. Concentration Pulse Chromatographic Methods Used in This Study

	MVV−CPM (Modified Van der Vlist and Van der Meijden−Concentration Pulse Method)[26]
four-parameter function	$K_p = A_0 + A_1y_1 + A_2y_1^2 + A_3y_1^3$
isotherm slope functions	$dn^a{}_1/dP_1 = B_0 + B_1y_1 + B_2y_1^2 \quad dn^a{}_2/dP_2 = C_0 + C_1y_1 + C_2y_1^2$
binary isotherm functions	$n^a{}_1 = \left(B_0y_1 + B_1y_1^2/2 + B_2y_1^3/3\right)P \quad n^a{}_2 = \left[C_0(1-y_1) + C_1(1-y_1^2)/2 + C_2(1-y_1^3)/3\right]P$
	MTT−CPM (Modified Triebe and Tezel−Concentration Pulse Method)[44,31]
five-parameter function	$K_p = A_{-1}(\beta + y_1) + A_0 + A_1/(\beta + y_1) + A_2/(\beta + y_1)^2$
isotherm slope functions	$dn^a{}_1/dP_1 = B_0 + B_1/(\beta + y_1) + B_2/(\beta + y_1)^2 \quad dn^a{}_2/dP_2 = C_0 + C_1/(\beta + y_1) + C_2/(\beta + y_1)^2$
binary isotherm functions	$n^a{}_1 = \left[B_0y_1 + B_1\ln\left[(\beta + y_1)/\beta\right] + B_2y_1/(\beta(\beta + y_1))\right]P$
	$n^a{}_2 = \left[C_0(1-y_1) - C_1\ln\left[(\beta + y_1)/(\beta + 1)\right] + C_2(1-y_1)/[(\beta + 1)(\beta + y_1)]\right]P$
	HT−CPM (Harlick and Tezel−Concentration Pulse Method)[9,31]
five-parameter function	$K_p = A_1 + A_2y_1 + A_3y_1^2 + A_4\ \ln\lvert y_1 + \lambda\rvert$
isotherm slope functions	$dn^a{}_1/dP_1 = B_1 + 2B_2y_1 + B_3/\lvert y_1 + \lambda\rvert \quad dn^a{}_2/dP_2 = C_1 + 2C_2y_1 + C_3/\lvert y_1 + \lambda\rvert$
binary isotherm functions	$n^a{}_1 = [B_1y_1 + B_2y_1^2 + B_3\ln\lvert(y_1 + \lambda)/\lambda\rvert]P \quad n^a{}_2 = [C_1(1-y_1) + C_2(1-y_1^2) - C_3\ln\lvert(y_1 + \lambda)/(1 + \lambda)\rvert]P$

loading; and R is the gas constant. The saturation capacity of the Sips and Toth equations can either be taken as constant or it can take the following temperature dependence

$$n_m{}^a = n_{m0}^a e^{\chi\left(1-\frac{T}{T_0}\right)} \tag{2}$$

where n_{m0}^a is the saturation capacity (maximum amount adsorbed) at the reference temperature T_0 and χ is a constant parameter. The exponent n of the Sips equation may take the following form

$$\frac{1}{n} = \frac{1}{n_0} + \alpha\left(1 - \frac{T_0}{T}\right) \tag{3}$$

and the form of the exponent n of the Toth equation can be

$$n = n_0 + \alpha\left(1 - \frac{T_0}{T}\right) \tag{4}$$

where n_0 is the parameter n at the reference temperature T_0 and α is a constant.[33]

Models for mixed-gas adsorption should be capable of predicting the equilibrium amount adsorbed from pure gas isotherms. The simplest theory for the binary system is the extended Langmuir model.[39]

$$\theta_A = \frac{n^a{}_A}{n^a{}_{mA}} = \frac{B_AP_A}{1 + B_AP_A + B_BP_B} \tag{5}$$

where subscripts A and B refer to adsorbates A and B, respectively.

The dual-site extended Langmuir adsorption isotherm was derived from the extended Langmuir model.[40] The Sips equation for the pure component adsorption isotherm may be extended to binary systems, as well.[41,42]

Some thermodynamic equations associated with the ideal solution derive the ideal adsorbed solution theory, which can be used to get the isotherm of a binary system assuming the mixture behaves as an ideal solution.[25]

In the concentration pulse chromatographic technique, dimensionless Henry's Law constant, K, can be calculated from the corrected first moment of the response peak as follows.[14,15,31,43]

$$\mu = \frac{\int_0^\infty c(t-\mu_D)dt}{\int_0^\infty cdt} = \frac{L}{v}\left[1 + \frac{(1-\varepsilon)K}{\varepsilon}\right] \tag{6}$$

where t is the time; c is the adsorbate concentration measured at the outlet of the column; L is the column length; ϵ is the bed porosity; v is the interstitial fluid velocity; K is the dimensionless Henry's law adsorption equilibrium constant; and μ_D is the dead time. The dimensionless Henry's law constants, K, can be converted to a dimensional form, K_p.[15]

The K_p value is related to the slopes of the isotherms of the components in the carrier gas mixture. For a binary mixture, the relationship is given as follows[27]

$$K_p = (1 - y_1)\frac{dn^a{}_1}{dP_1} + y_1\frac{dn^a{}_2}{dP_2} \tag{7}$$

where $dn^a{}_1/dP_1$ and $dn^a{}_2/dP_2$ are the slopes of the adsorption isotherms for components 1 and 2, respectively.

For binary isotherms, both components in the mixed carrier gas are adsorbed, and $dn^a{}_2/dP_2$ in the last term of eq 7 is not constant. The experimental K_p data represent the combined contribution of both components to the isotherms. The interpretation of the binary K_p data has been treated by several methods[9,26,31,44] shown in Table 1.

The following objective function is defined to minimize the sum of the square residuals (SSR) with respect to the experimental values for the determination of B and C parameters (see Table 1) to obtain the binary isotherms

$$\mathrm{SSR} = \sum_{y_1=0}^{y_1=1}(K_{p,\mathrm{experiment}} - K_{p,\mathrm{equation}})^2 \tag{8}$$

The minimization of the sum of the square residuals (SSR) could not be performed with only the experimental data points, since a number of possible solutions could exist for B and C coefficients. Four constraints are imposed on the system, to ensure that the solution reflects what is physically occurring. Two of these constraints are the two end points of the concentration range, which should coincide with the pure isotherms. The other two constraints come from the fact that the binary isotherm slopes should always be positive across the entire range of y_1; i.e., no maximum should be seen in the isotherms.[45]

By using these constraints to bind the objective function (eq 8), a constrained nonlinear regression could be performed to determine the B and C parameters. The K curve is defined from the RHS of eq 7, and the binary isotherms are calculated by binary isotherm functions in Table 1 by using B and C coefficients.

The thermodynamics of pure and binary gas adsorption systems has been extensively studied using the Gibbsian surface excess (GSE) model.[46–48] For binary gas adsorption systems, it has been used to develop several relationships for checking both the thermodynamic consistency between pure and binary gas equilibrium adsorption data and the internal thermodynamic consistency of the binary adsorption data itself. These relation-

Table 2. Details of the Adsorbent Used in This Study

type	silicalite
commercial name	MOLSIV adsorbents
commercial number	HISIV 3000
particle form received	1/16 in. extrudate as received
size used in the column (diameter)	crushed to 20 × 60 mesh
content of binder	20 wt %
particle density	1.131 g·cm^{-3}
void fraction	0.39
supplier	Universal Oil Products, Des Plaines, IL, USA

Table 3. Details of Sample Gases Used in This Study

gases	Grade	Purity	Supplier
CO_2	bone dry 3.0	99.9 %	Praxair Inc., Ottawa
N_2	ultra high purity 5.0	99.999 %	Praxair Inc., Ottawa
He	ultra high purity 5.0	99.999 %	Praxair Inc., Ottawa

ships of integral and differential consistency tests have been developed for pure and binary gas adsorption data. The integral test requires the measurement of both pure gas adsorption isotherms and binary gas adsorption isotherms shown below.[49]

$$\left(-\int_0^P \frac{n^{a0}_2}{P}dP\right)-\left(-\int_0^P \frac{n^{a0}_1}{P}dP\right)=\int_0^1 \frac{n^a_1(1-y_1)-n^a_2 y_1}{y_1(1-y_1)}dy_1 \quad (9)$$

where $n^{a0}{}_1$ and $n^{a0}{}_2$ are the amount adsorbed of components 1 and 2, respectively, in the pure gas systems; P is both the pressure of pure gas systems and the total pressure of the binary system; $n^a{}_1$ and $n^a{}_2$ are the amounts adsorbed of components 1 and 2, respectively, in the binary system; and y_1 is the mole fraction of component 1 in the binary gas system. The two terms on the left-hand side of eq 9 are the potentials of adsorption at P and T for pure gases 2 and 1, respectively. They can be estimated as a function of P at constant T using the pure gas adsorption isotherms. Thus, the quantity on the left side at any given values of P and T can be evaluated from the pure gas adsorption isotherms of the components of a binary gas mixture. The quantity on the right side at any given values of P and T can be evaluated using the binary gas adsorption isotherm at constant P and T. These two independently measured quantities must be equal; this equality forms the basis for the integral consistency test between pure and binary gas equilibrium adsorption data.

Experimental Section

The details of the volumetric system, concentration pulse chromatography technique, and numerical methods are given in our earlier paper.[50] The details about adsorbent and sample gases used in the experiments are listed in Tables 2 and 3, respectively. It should be noted that the values of adsorption capacities obtained from experiments were corrected with respect to the binder, assuming that the binder has negligible adsorption. Experimental and numerical errors are determined to be less than 5 %.

Results and Discussion

Pure Gas Adsorption. Equilibrium isotherm data for CO_2 and N_2 on silicalite pellets were obtained at three different temperatures for pressures up to 5 bar and are given in Figure 1 as data points. The curves going through the data points are regressed with Toth isotherm models at the corresponding temperature. The numbered curves are data from the literature for comparison with the present study. All the values of adsorption capacity obtained from experiments in this work were corrected with respect to the binder with the composition of the binder given by the manufacturer, assuming that the binder does not have any adsorption capacity. When the results are compared to the literature in Figure 1, it can be seen that adsorption capacities are in good agreement qualitatively for CO_2, considering different temperatures. They are slightly higher than those given in the literature for N_2, which may be due to different suppliers.

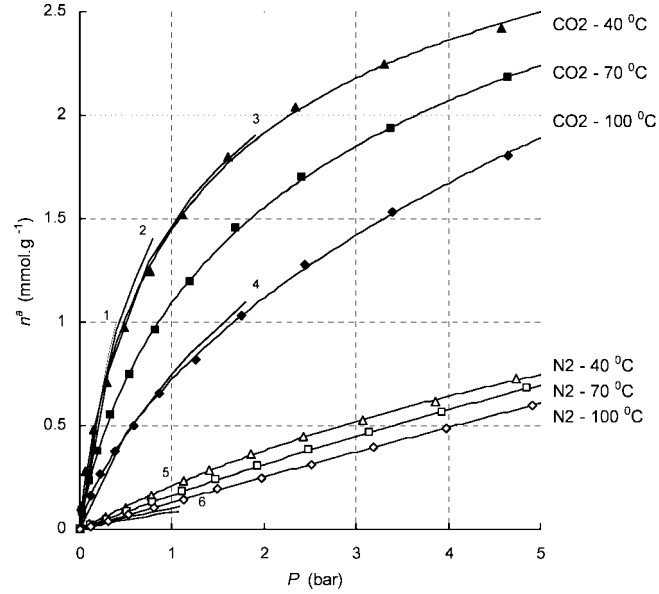

Figure 1. Isotherms for CO_2 and N_2 on silicalite: the points are experimental data, and the curves are Toth isotherms. The numbered curves indicate comparisons with the literature: **1**, CO_2, 25 °C;[51] **2**, CO_2, 31 °C;[52] **3**, CO_2, 32 °C;[53] **4**, CO_2, 80 °C;[53] **5**, N_2, 23 °C;[52] **6**, N_2, 61 °C;[52] **7**, N_2, 72 °C.[52]

Adsorption capacity increases with decreasing temperature for both of the adsorbates since physical adsorption is always exothermic. CO_2 is adsorbed more than N_2 since the interactive forces between CO_2 and silicalite are bigger than those for N_2. Higher polarizability and quadrupole moment of carbon dioxide make it much more interactive than N_2. At low pressure, the slopes of the isotherms for carbon dioxide are very high, and then the slopes decrease rather fast with increasing pressure as the adsorbent sample approaches saturation. However, the slopes of the isotherms of nitrogen hardly decrease as pressure increases, isotherms being more linear at high temperatures.

By using nonlinear regressions, the parameters of different models were obtained, and corresponding parameters are shown in Table 4. For gauging the quality of the nonlinear regressions obtained from the different models used, the RMS (root-mean-square) deviations ($[\Sigma(n^a_{data} - n^a_{curve})^2/n]^{0.5}$) are used and shown in Table 4. When two-parameter models, Langmuir and Freundlich, are compared, Langmuir is better than Freundlich. When three- or four-parameter models were considered, it was observed that all of them, Toth, Sips, Flory−Huggins vacancy solution theory (VST), multisite−Langmuir, and dual-site−Langmuir models are better than the two-parameter models because of their increased flexibility.

The temperature dependent forms of the Toth and Sips equations were also used for description of adsorption equilibrium data at various temperatures. In eq 2, χ can be taken as 0 or a parameter. According to our data, all the values of χ obtained are 0 as a parameter for the temperature dependent form of the Toth equation. For the temperature dependent form

of the Sips equation, some values of χ obtained are 0 and some are not. However, there is little difference between them for modeling the isotherms. For one less parameter, we took χ as 0. In other words, the saturation capacities of the temperature dependent isotherm equations (both Sips and Toth) were constant, that is $n^a_m = n^a_{m0}$. Using the data at the three temperatures simultaneously in the fitting of both temperature dependent isotherms (Sips and Toth equations), optimal parameters shown in Table 5 were obtained. The parameters and RMS deviations at the three temperatures are listed in Table 4. From the parameters given in Table 5 for temperature dependent Toth and Sips isotherms, the experimental data are extended to other temperature and pressures.

The primary requirement for an economic separation process is an adsorbent with sufficiently high selectivity, capacity, and life. The selectivity may depend on a difference in either adsorption kinetics or adsorption equilibrium. Most of the adsorption processes in current use depend on equilibrium selectivity. In considering such processes, it is convenient to define an ideal adsorption separation factor

$$\alpha_{A/B} = \frac{x_A/x_B}{y_A/y_B} \tag{10}$$

where x_A, x_B, y_A, and y_B are, respectively, the mole fractions of components A and B in adsorbed and fluid phases at equilibrium. If the isotherms are linear or pressure is small enough for the isotherms to keep in the linear range, ideally, the separation factor is given simply by the ratio of the amounts adsorbed in pure components

$$\alpha_{i,A/B} = \frac{n^a_A}{n^a_B} \tag{11}$$

where n^a_A and n^a_B are the amounts adsorbed of components A and B. These equilibrium separation factors that are calculated directly from pure component data are shown as a function of pressure and temperature in Figure 2. The temperature dependent Toth model was used for the extension of the data to other temperatures and pressures for this figure. As can be seen from these results, both pressure and temperature are very important

Table 4. Parameters and RMS Deviations of Adsorption Models by Nonlinear Regressions

			CO_2			N_2		
models	equations	parameters	40 °C	70 °C	100 °C	40 °C	70 °C	100 °C
Langmuir (2 param.)	$n^a = n^a_m BP/(1 + BP)$	B (bar^{-1})	1.089	0.649	0.332	0.111	0.045	0.013
		n^a_m ($mmol \cdot g^{-1}$)	2.858	2.834	2.911	2.094	3.765	9.993
		RMS ($mmol \cdot g^{-1}$)	0.050	0.040	0.038	0.004	0.002	0.002
Freundlich (2 param.)	$n^a = kP^{1/n}$	k ($mmol \cdot g^{-1} \cdot bar^{-1/n}$)	1.340	1.035	0.713	0.212	0.166	0.129
		n (dimensionless)	2.295	1.938	1.616	1.247	1.112	1.037
		RMS ($mmol \cdot g^{-1}$)	0.106	0.067	0.022	0.011	0.005	0.002
Sips (Langmuir− Freundlich) (3 param.)	$n^a = n^a_m(BP)^{1/n}/[1 + (BP)^{1/n}]$	B (bar^{-1})	0.675	0.337	0.065	0.118	0.046	0.0006
		n^a_m ($mmol \cdot g^{-1}$)	3.431	3.697	6.240	2.014	3.722	176.2
		n (dimensionless)	1.256	1.249	1.349	0.989	0.999	1.035
		RMS ($mmol \cdot g^{-1}$)	0.021	0.012	0.009	0.004	0.002	0.002
Toth (3 param.)	$n^a = n^a_m BP/[1 + (BP)^n]^{1/n}$	B (bar^{-1})	1.397	0.678	0.100	0.109	0.041	0.002
		n^a_m ($mmol \cdot g^{-1}$)	3.903	4.885	38.98	2.125	4.207	84.58
		n (dimensionless)	0.604	0.537	0.260	0.990	0.951	0.598
		RMS ($mmol \cdot g^{-1}$)	0.028	0.013	0.011	0.003	0.002	0.002
Flory−Huggins VST (3 param.)	$P = \left(\frac{1}{B} \cdot \frac{n^a}{1 - \frac{n^a}{n^a_m}}\right) \exp\left(\frac{\alpha^2 \cdot \frac{n^a}{n^a_m}}{1 + \alpha^2 \cdot \frac{n^a}{n^a_m}}\right)$	B ($mmol \cdot g^{-1} \cdot bar^{-1}$)	3.874	2.608	1.280	0.242	0.172	0.129
		n^a_m ($mmol \cdot g^{-1}$)	3.082	3.498	5.969	3.453	32.29	10.31
		α_{1v} (dimensionless)	1.020	1.525	2.123	1.161	3.085	4×10^{-7}
		RMS ($mmol \cdot g^{-1}$)	0.032	0.014	0.019	0.004	0.002	0.002
multisite−Langmuir (3 param.)	$BP = n^a/n^a_m/\left(1 - n^a/n^a_m\right)^n$	B (bar^{-1})	1.002	0.341	0.014	0.013	0.006	0.004
		n^a_m ($mmol \cdot g^{-1}$)	3.322	6.567	78.01	18.03	30.91	34.74
		n (dimensionless)	1.412	3.881	43.90	10.97	9.177	3.489
		RMS ($mmol \cdot g^{-1}$)	0.049	0.019	0.027	0.003	0.002	0.002
dual-site−Langmuir (4 param.)	$n^a = \frac{n^a_{m1} B_1 P}{1 + B_1 P} + \frac{n^a_{m2} B_2 P}{1 + B_2 P}$	B_1 (bar^{-1})	0.782	0.393	0.190	0.009	0.045	0.013
		n^a_{m1} ($mmol \cdot g^{-1}$)	2.822	2.904	3.492	3.570	3.765	9.849
		B_2 (bar^{-1})	36.44	7.003	11.00	0.140	0.919	0.004
		n^a_{m2} ($mmol \cdot g^{-1}$)	0.217	0.305	0.173	1.442	0	0.0254
		RMS ($mmol \cdot g^{-1}$)	0.012	0.019	0.027	0.004	0.002	0.002
temperature dependent Sips	$n^a = n^a_m(BP)^{1/n}/[1 + (BP)^{1/n}]$	B (bar^{-1})	0.594	0.343	0.212	0.075	0.070	0.065
		n^a_m ($mmol \cdot g^{-1}$)	3.614	3.614	3.614	2.694	2.694	2.694
		n (dimensionless)	1.321	1.223	1.149	1.046	0.968	0.907
		RMS ($mmol \cdot g^{-1}$)	0.026	0.026	0.026	0.006	0.006	0.006
temperature dependent Toth	$n^a = n^a_m BP/[1 + (BP)^n]^{1/n}$	B (bar^{-1})	1.617	0.640	0.285	0.122	0.092	0.172
		n^a_m ($mmol \cdot g^{-1}$)	4.649	4.649	4.649	1.801	1.801	1.801
		n (dimensionless)	0.496	0.570	0.635	1.155	1.497	1.804
		RMS ($mmol \cdot g^{-1}$)	0.031	0.015	0.024	0.005	0.004	0.004

Table 5. Optimal Parameters for the Temperature Dependent Toth and Sips Equations for a Reference Temperature T_0 = 40 °C

adsorbate	parameters	units	temperature dependent Toth	temperature dependent Sips
CO_2	χ	dimensionless	0	0
	n^a_{m0}	mmol·g^{-1}	4.649	3.614
	B_0	bar^{-1}	1.660	0.603
	Q/RT_0	dimensionless	10.87	6.439
	n_0	dimensionless	0.494	1.324
	α	dimensionless	0.869	0.708
N_2	χ	dimensionless	0	0
	n^a_{m0}	mmol·g^{-1}	1.801	2.694
	B_0	bar^{-1}	0.123	0.075
	Q/RT_0	dimensionless	3.278	0.881
	n_0	dimensionless	1.152	1.047
	α	dimensionless	4.000	0.903

for the separation. In general, separation factors increase with decreasing pressure and/or temperature. It is difficult to separate the system at high temperature and/or high pressure.

The PSA process can be carried out at room temperature and in the range of pressures between vacuum and 1 bar. If it is done at a temperature higher than 100 °C and in the range of pressure higher than 1 bar, the expected results become worse as the ideal separation factor is dropped down to 6 in Figure 2. For a TSA process, it can be done under a vacuum as low a pressure as possible and at temperatures as low as possible. Since flue gas temperatures are generally rather high, temperature conditions should be considered.

Binary Isotherms. After regenerating the silicalite adsorbent, K_p values were determined by increasing the CO_2 mole fraction in CO_2-CH_4 carrier gas from 0 % up to 100 %. The samples were injected after attaining equilibrium for each concentration change of the carrier gas by noting that the baseline of the response would be steady. The K_p values, as well as their corresponding curve fits for HT−CPM, MTT−CPM, and MVV−CPM, as a function of the gas composition are given in Figure 3. Figure 3b gives the same data as Figure 3a in the low K_p data range to be able to see the curve fits much better. As

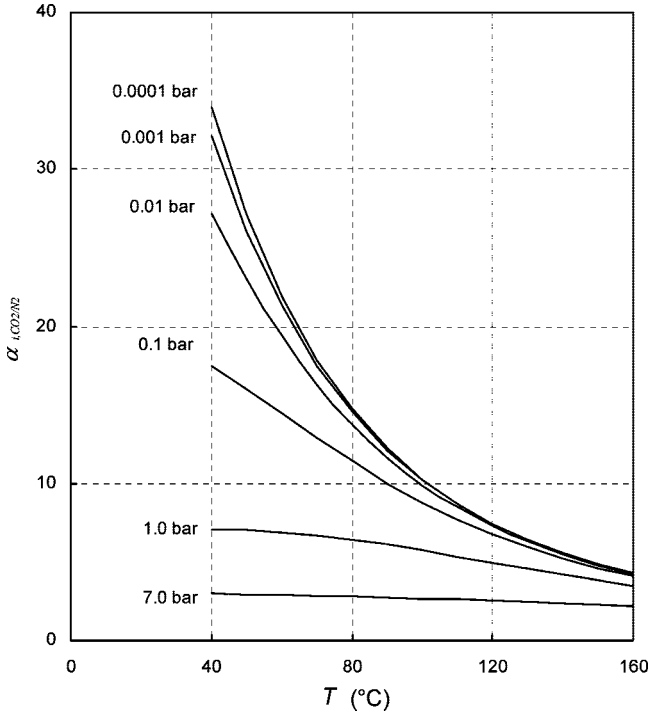

Figure 2. Ideal separation factors for CO_2/N_2, on silicalite.

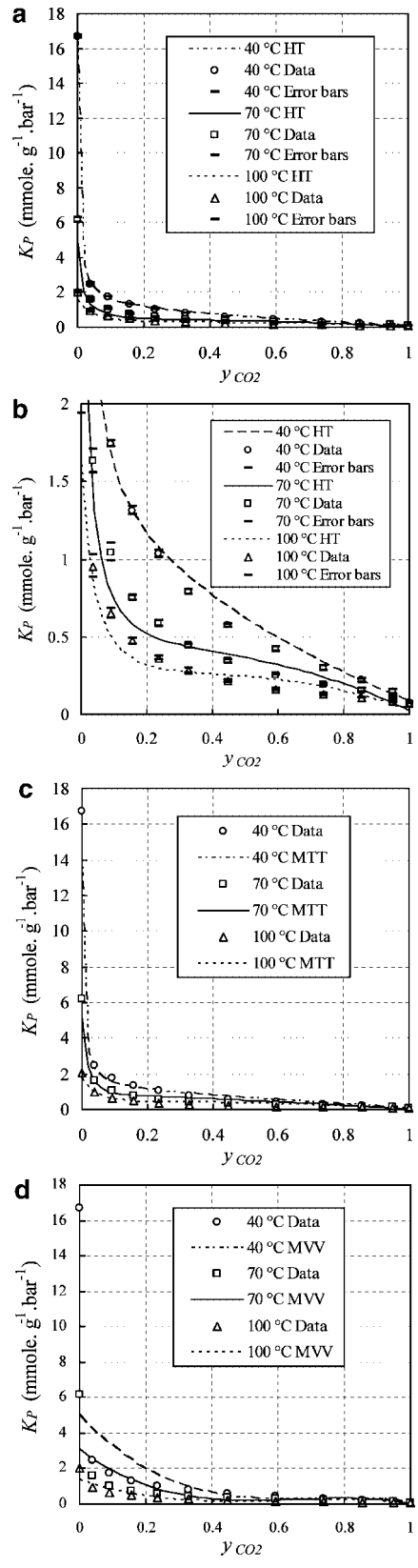

Figure 3. (a) Regressions for CO_2/N_2, binary K_p, with silicalite by HT−CPM at different carrier gas compositions at 1 bar total pressure. (b) Regressions for CO_2/N_2, binary K_p, with silicalite by HT−CPM at different carrier gas compositions at 1 bar total pressure showing low K_p values ranging between (0 and 2) mmol·g^{-1}·bar^{-1}. (c) Regressions for CO_2/N_2, binary K_p, with silicalite by MTT−CPM at different carrier gas compositions at 1 bar total pressure. (d) Regressions for CO_2/N_2, binary K_p, with silicalite by MVV−CPM at different carrier gas compositions at 1 bar total pressure.

Table 6. RMS Deviations ($[\Sigma(K_{p,\text{data}} - K_{p,\text{curve}})^2/n]^{0.5}$) in mmol·g^{-1}·bar^{-1} of Concentration Pulse Chromatographic Methods for the CO_2−N_2 Binary System on Silicalite

CPM	40 °C	70 °C	100 °C
HT	0.060	0.080	0.059
MTT	0.070	0.111	0.078
MVV	3.303	0.939	0.197

can be seen from this figure, the best fit was obtained with the HT−CPM. As was proven before,[31,54] this method is a more versatile method, which would accommodate more nonideal systems, where the adsorption capacities of the two adsorbates are very different from each other.

To quantify and compare the nonlinear regressions for these three concentration pulse methods, the RMS (root-mean-square) deviations ($[\Sigma(n^a_{\text{data}} - n^a_{\text{curve}})^2/n]^{0.5}$) were used and shown in Table 6. It was observed that the best fit was actually given by the HT−CPM method. Therefore, the HT−CPM, shown with error bars in Figures 3a and 3b, was used to describe these systems for our further study of this binary system.

The binary isotherms for CO_2−N_2 with silicalite at 1 bar total pressure were obtained at three temperatures and are given in Figure 4 for (40, 70, and 100) °C for different compositions of the gas mixture. When y_{CO2} increases, the CO_2 adsorption capacity, n^a_{CO2}, increases and the N_2 adsorption capacity, n^a_{N2}, decreases. The total adsorbed capacity, n^a_{total}, increases as an increase of n^a_{CO2} is more than the decrease of n^a_{N2}. At the beginning, n^a_{N2} decreases very fast while n^a_{CO2} increases rapidly. When y_{CO2} is higher than 0.2, n^a_{N2} is close to zero and approaches zero. For flue gas applications, y_{CO2} is around 0.15, and the CO_2 adsorption capacity is much higher than that of N_2; therefore, this trend in adsorption capacities for N_2 and CO_2 is very promising for silicalite as an adsorbent for applications in CO_2 removal from air. n^a_{CO2}, n^a_{N2}, and n^a_{total} increase with decreasing temperatures since adsorption is exothermic, so temperature is a very important factor. For practical applications, the separation process can be controlled at low temperature to attain good adsorption capacity.

To predict the binary adsorption behavior from pure gas systems, the following six models were used and compared to the experimental binary adsorption behavior: extended Langmuir, extended dual-site Langmuir, ideal adsorbed solution theory, statistical model, extended sips, and Flory−Huggins of vacancy solution theory. For estimating and comparing the quality of the six binary model predictions, the RMS deviations from the binary experimental data ($[\Sigma(n^a_{\text{data}} - n^a_{\text{curve}})^2/n]^{0.5}$) were used and are listed in Table 7. It was observed that all the six prediction models are similar, and there is a rather big difference between the predicted and the experimental isotherms. Therefore, none of the six models can describe the real binary system accurately and they can be used only for rough estimation for the binary system when there are no binary data available. In Figure 4, experimental binary isotherms are compared with their counterparts predicted by the statistical model isotherms. Since all predictions were similar to each other, only the statistical model was shown in this figure as an example. As can be seen from these comparisons, the predicted isotherms mostly over predict the real ones at all temperatures studied.

The x−y phase diagrams at different temperatures studied are shown in Figure 5, together with comparison with the predictions from the extended Langmuir isotherms, using the pure component isotherms. Within the temperature range studied, lower temperature data gave better separation, since the curve was the furthest from the 45° line. Realistic experimental data gave better separation than the ideal extended Langmuir predicted.

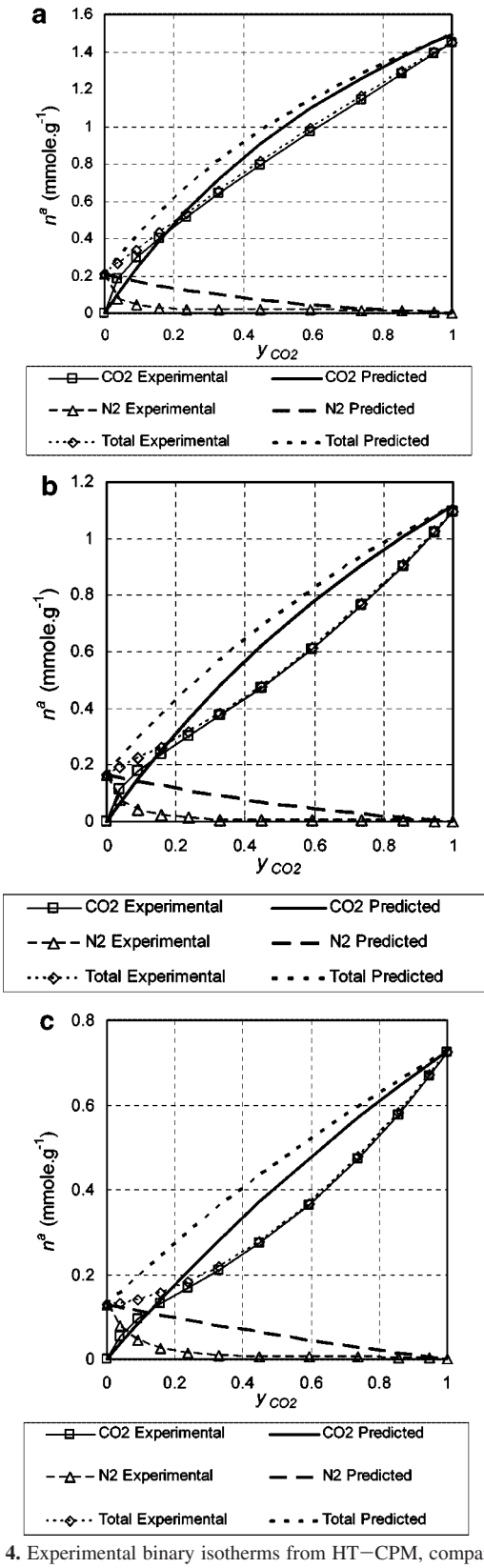

Figure 4. Experimental binary isotherms from HT−CPM, compared with predicted binary isotherms from the statistical model for CO_2/N_2 with silicalite at 1 bar total pressure. (a) 40 °C. (b) 70 °C. (c) 100 °C.

In Figure 5, the experimental x−y diagram given at 40 °C by Harlick and Tezel[9] in the literature for ZSM-5-30 under the same conditions is compared with the ones obtained in this study. Silicalite and ZSM-5 have the same structure. ZSM-5-

Table 7. RMS Deviations ($[\Sigma(n^a_{data} - n^a_{curve})^2/n]^{0.5}$) in mmol·g^{-1} of Predicted Isotherms from the Experimental Ones for the CO_2-N_2 Binary System on Silicalite

models	capacity	40 °C	70 °C	100 °C
extended Langmuir	n^a_{CO2}	0.081	0.103	0.068
	n^a_{N2}	0.086	0.071	0.054
	n^a_{total}	0.122	0.150	0.108
extended dual-site Langmuir	n^a_{CO2}	0.094	0.101	0.096
	n^a_{N2}	0.016	0.075	0.055
	n^a_{total}	0.101	0.159	0.147
extended Sips	n^a_{CO2}	0.042	0.057	0.140
	n^a_{N2}	0.091	0.075	0.042
	n^a_{total}	0.115	0.109	0.131
ideal adsorbed solution theory	n^a_{CO2}	0.084	0.102	0.066
	n^a_{N2}	0.083	0.072	0.056
	n^a_{total}	0.122	0.150	0.108
Flory−Huggins VST	n^a_{CO2}	0.081	0.359	0.091
	n^a_{N2}	0.077	0.206	0.064
	n^a_{total}	0.127	0.563	0.147
statistical method	n^a_{CO2}	0.084	0.102	0.066
	n^a_{N2}	0.081	0.071	0.055
	n^a_{total}	0.119	0.147	0.107

30 adsorbent had a different Si/Al ratio indicated by the last number in the code of the adsorbent, 30, as opposed to the silicalite for which this ratio is in the thousands. Since the only difference between the adsorbent studied in this work and Harlick and Tezel's adsorbent was the Si/Al ratio, it is concluded that this ratio influences the binary behavior of the CO_2-CH_4 gas mixture slightly, and the separation is better when this ratio is smaller.

The equilibrium separation factors are calculated from the binary isotherms obtained, using eq 10, and plotted against y_{CO2} in Figure 6 at three different temperatures for the CO_2/N_2 and silicalite system. The selectivity is good, and temperature has a big influence on the separation factor. The selectivity increases with increasing y_{CO2} and decreasing temperature when CO_2 concentration in the mixture is in the range between 10 % and 20 % for flue gas applications. These experimental equilibrium separation factors are compared to the ones predicted by using pure component isotherms in Figure 6. As can be observed from this figure, the experimental separation factors are higher, and

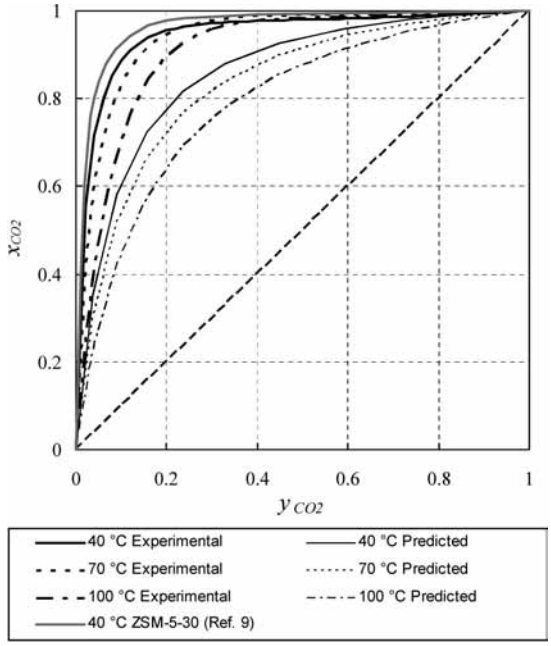

Figure 5. $x-y$ diagrams for CO_2/N_2 binary systems with silicalite at 1 bar total pressure and comparison with the literature values for ZSM-5-30.[9]

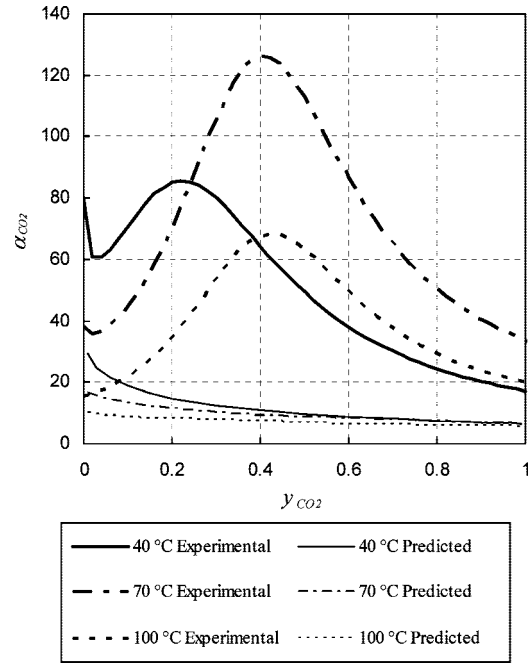

Figure 6. Equilibrium separation factor curves for the CO_2/N_2 and silicalite system at different temperatures studied: experimental from binary adsorption isotherms and predicted from pure gas isotherms.

they show a maximum at all temperatures studied. The predicted ones decline steadily as CO_2 composition in the gas phase increases. This difference in binary behavior comes from competitive adsorption in the real binary system, which can not be predicted from the ideal mixture behavior. Therefore, predicted separation factors can only be used to do rough estimations in the absence of binary experimental data.

According to eq 9, the integral thermodynamic consistency test between pure and binary equilibrium adsorption data is shown in Table 8. For the binary systems, the integrands of the right side as functions of y_1 (y_{CO2}) can be plotted, and the areas under these curves between y_1 (y_{CO2}) = 0 and y_1 (y_{CO2}) = 1 are listed in this table. For pure systems, the integrands of the left side as functions of P can be plotted, and the areas under these curves between P = 0 bar and P = 1 bar are listed in Table 8. It should be pointed out that the ranges of pressure of the pure systems are the same as the ranges of the partial pressures of the two components as the total pressure of binary system is 1 bar.

In Table 8, it can be seen that the integral thermodynamic consistency test is obeyed fairly well by the binary CO_2-N_2 adsorption data on silicalite at 40 °C. At (70 and 100) °C, the discrepancy increases. The results of the integral thermodynamic consistency test match the results of predicting the adsorption behavior of the binary system from pure gas systems in Figure 4 very well. At low temperature, the thermodynamic consistency is good, so the difference of predicting the adsorption behavior of the binary system from pure gas systems is small. At high temperature, the thermodynamic consistency is less satisfied, so it is impossible to predict the adsorption behavior of the binary system from pure gas isotherms accurately. Thus, we recommend that one key requirement for predicting the adsorption behavior of the binary system from pure gas systems is that they satisfy the integral thermodynamic consistency tests between pure and binary gas adsorption equilibria.

Conclusions

1. According to the pure gas isotherm data on silicalite, carbon dioxide is adsorbed much more than nitrogen.

Table 8. Integral Thermodynamic Consistency Test between Pure and Binary Carbon Dioxide (1) + Nitrogen (2) Equilibrium Adsorption Data on Silicalite Using Equation 9

temperature	°C	40	70	100
RHS: $\int_0^1 [n^a{}_1(1-y_1) - n^a{}_2 y_1] / [y_1(1-y_1)] dy_1$	mmol·g^{-1}	2.1231	1.3003	0.7166
1st term in LHS: $\int_0^1 \left(n^{a0}_1 / P\right) dP$	mmol·g^{-1}	2.3084	1.5809	1.0193
2nd term in LHS: $\int_0^1 \left(n^{a0}_2 / P\right) dP$	mmol·g^{-1}	0.2200	0.1671	0.1298
LHS: $\int_0^1 \left(n^{a0}_1 / P\right) dP - \int_0^1 \left(n^{a0}_2 / P\right) dP$	mmol·g^{-1}	2.0883	1.4136	0.8895
1(LHS − RHS) / RHS|·100	%	1.64	8.72	24.13

2. Temperature dependent Toth is a useful model for extrapolation and/or interpolation to predict adsorption capacities at other temperatures and pressures.

3. Among the three concentration pulse chromatographic methods used, the HT−CPM is the best one, the MTT−CPM is very good, and the MVV−CPM is not satisfactory for describing the binary behavior of CO_2/N_2 with silicalite.

4. The adsorption capacities for N_2 and CO_2 are very promising for silicalite as an adsorbent in applications in CO_2 removal from air for flue gas applications.

5. $n^a{}_{CO2}$, $n^a{}_{N2}$, and $n^a{}_{total}$ increase with decreasing temperature. Therefore, temperature is a very important factor for the separation of this system, particularly when y_{CO2} is very low.

6. For the prediction of the CO_2/N_2 binary system, Flory−Huggins Vacancy Solution Theory can not be used, at all. The Extended Langmuir, Extended Dual-Site Langmuir, Ideal Adsorbed Solution Theory, Statistical Model, and Extended Sips models cannot describe the real binary system accurately, either, and they can only be used at low temperatures or for rough estimation when the binary data are not available.

7. The selectivity is excellent for the CO_2/N_2 binary system with silicalite.

8. The CO_2-N_2 binary adsorption data on silicalite at low temperature satisfy the integral thermodynamic consistency test fairly well. The thermodynamic consistency is less satisfied as temperature increases.

Nomenclature

B = adsorption affinity constant, usually bar^{-1} (units depending on models)

B_0 = adsorption affinity constant at some reference temperature, bar^{-1}

B_1 = adsorption affinity constant in site 1, bar^{-1}

B_2 = adsorption affinity constant in site 2, bar^{-1}

K = dimensionless Henry's law constant, dimensionless

K_p = dimensional Henry's law constant, mmol·g^{-1}·bar^{-1}

n = adsorption exponent or number of active sites, dimensionless

n_0 = adsorption exponent at some reference temperature, dimensionless

n^a = amount adsorbed, mmol·g^{-1}

$n^a{}_A$ = amount adsorbed of component A, mmol·g^{-1}

$n^a{}_B$ = amount adsorbed of component B, mmol·g^{-1}

$n^a{}_1$ = amount adsorbed of component 1, mmol·g^{-1}

$n^a{}_2$ = amount adsorbed of component 2, mmol·g^{-1}

$n^{a0}{}_1$ = amount adsorbed of component 1 in the pure system, mmol·g^{-1}

$n^{a0}{}_2$ = amount adsorbed of component 2 in the pure system, mmol·g^{-1}

$n^a{}_m$ = adsorption saturation capacity or maximum amount adsorbed, mmol·g^{-1}

$n^a{}_{m0}$ = adsorption saturation capacity or maximum amount adsorbed at some reference temperature, mmol·g^{-1}

$n^a{}_{m1}$ = adsorption saturation capacity or maximum amount adsorbed in site 1, mmol·g^{-1}

$n^a{}_{m2}$ = adsorption saturation capacity or maximum amount adsorbed in site 2, mmol·g^{-1}

P = (total) pressure, bar

P_1 = pressure of component 1, bar

P_2 = pressure of component 2, bar

P_A = pressure of component A, bar

P_B = pressure of component B, bar

Q = isosteric heat, J·mol^{-1}

R = gas constant, 8.314 J·K^{-1}·mol^{-1}

T = temperature, K

T_0 = reference temperature, K

x = mole fraction in adsorbed phase at equilibrium, dimensionless

x_A = mole fraction of component A in adsorbed phase at equilibrium, dimensionless

x_B = mole fraction of component B in adsorbed phase at equilibrium, dimensionless

y = mole fraction in fluid phase at equilibrium, dimensionless

y_A = mole fraction of component A in fluid phase at equilibrium, dimensionless

y_B = mole fraction of component B in fluid phase at equilibrium, dimensionless

y_1 = mole fraction of component 1 in fluid phase at equilibrium, dimensionless

Greek letters

α = adsorption constant, adsorption separation factor, dimensionless

$\alpha_{A/B}$ = adsorption separation factor (the ratio of component A over component B), dimensionless

$\alpha_{i,A/B}$ = ideal adsorption separation factor (the ratio of component A over component B), dimensionless

θ = fraction of monolayer coverage, dimensionless

χ = constant parameter, dimensionless

Abbreviations

CPM = concentration pulse method
DSL = dual-site Langmuir
GHG = greenhouse gases
GSE = Gibbsian surface excess
GWP = greenhouse warming potential
LFG = landfill gas
PSA = pressure swing adsorption
RMS = root-mean-square
SSR = sum of the square residuals
TCD = thermal conductivity detector
TSA = temperature swing adsorption
VST = vacancy solution theory

Literature Cited

(1) Cavenati, S.; Grande, C. A.; Rodrigues, A. E. Upgrade of Methane from Landfill Gas by Pressure Swing Adsorption. *Energy Fuels* **2005**, *19*, 2545–2555.

(2) Hansen, J.; Fung, I.; Lacis, A.; Riud, D.; Levedeff, J. S.; Ruedy, R.; Russell, G. Global Climate Changes as Forecast by Goddard Institute for Space Studies Three-Dimensional Model. *J. Geophys. Res.* **1988**, *93*, 9341–9364.

(3) Chue, K. T.; Kim, J. N.; Yoo, Y. J.; Cho, S. H.; Yang, R. T. Comparison of Activated Carbon and Zeolite 13X for CO_2 recovery from flue gas by Pressure Swing Adsorption. *Ind. Eng. Chem. Res.* **1995**, *34*, 591–598.
(4) Diagne, D.; Goto, M.; Hirose, T. New PSA Process with Intermediate Feed Inlet Position Operated with Dual Refluxes: Application to Carbon Dioxide Removal and Enrichment. *J. Chem. Eng. Jpn.* **1994**, *27*, 85–89.
(5) Dong, F.; Lou, H.; Kodama, A.; Goto, M.; Hirose, T. The Petlyuk PSA Process for the Separation of Ternary Gas Mixtures: Exemplification by Separation a Mixture of CO_2-CH_4-N_2. *Sep. Purif. Technol.* **1999**, *16*, 159–166.
(6) Dreisbach, F.; Staudt, R.; Keller, J. U. High Pressure Adsorption Data of Methane, Nitrogen, Carbon Dioxide and their Binary and Ternary Mixtures on Activated Carbon. *Adsorption* **1999**, *5*, 215–227.
(7) Gomes, V. G.; Yee, K. W. K. Pressure Swing Adsorption for Carbon Dioxide Sequestration from Exhaust Gases. *Sep. Purif. Technol.* **2002**, *28*, 161–171.
(8) Harlick, P. J. E.; Tezel, F. H.; Tremblay, A. Y. Carbon Dioxide Removal from Flue Gas Using Pressure Swing Adsorption: Modelling and Optimisation, Presented at the 51st Canadian Chemical Engineering Conference, Oct. 14−17, 2001.
(9) Harlick, P. J. E.; Tezel, F. H. CO_2-N_2 and CO_2-CH_4 Binary Adsorption Isotherms with H-ZSM-5: the Importance of Experimental Data Regression with the Concentration Pulse Method. *Can. J. Chem. Eng.* **2001**, *79*, 236–245.
(10) Harlick, P. J. E.; Tezel, F. H. Adsorption of Carbon Dioxide, Methane and Nitrogen: Pure and Binary Mixture Adsorption by H-ZSM-5 with SiO_2/Al_2O_3 Ratio of 30. *Sep. Sci. Technol.* **2002**, *37*, 33–60.
(11) Harlick, P. J. E.; Tezel, F. H. Adsorption of Carbon Dioxide, Methane and Nitrogen: Pure and Binary Mixture Adsorption for ZSM-5 with SiO_2/Al_2O_3 Ratio of 280. *Sep. Purif. Technol.* **2003**, *33*, 199–210.
(12) Hernandez-Huesca, R.; Diaz, L.; Aguilar-Armenta, G. Adsorption Equilibria and Kinetics of CO_2, CH_4 and N_2 in natural zeolites. *Sep. Purif. Technol.* **1999**, *15*, 163–173.
(13) Kikkinides, E. S.; Yang, R. T. Concentration and Recovery of CO_2 from Flue Gas by Pressure Swing Adsorption. *Ind. Eng. Chem. Res.* **1993**, *32*, 2714–2720.
(14) Li, P.; Tezel, F. H.; Chung, T-S N.; Kulprathipanja, S. Analysis of Adsorption Parameters by Concentration Pulse Chromatography, 55th Canadian Chemical Engineering Conference, Toronto, Canada, Oct. 16−19, 2005, 593.
(15) Li, P.; Tezel, F. H. Equilibrium and Kinetic Analysis of CO_2-N_2 Adsorption Separation by Concentration Pulse Chromatography. 40th IUPAC Congress, Beijing, P. R. China, Aug. 14−19, 2005, *p61*, 1-O−034
(16) Nishikawa, N. Removing and Recovering of CO_2. *J. Jpn. Inst. Energy* **1992**, *71*, 1090–1098.
(17) Pakseresht, S.; Kazemeini, M.; Akbarnejad, M. M. Equilibrium Isotherms for CO, CO_2, CH_4 and C_2H_4 on the 5A Molecular Sieve by a Simple Volumetric Apparatus. *Sep. Purif. Technol.* **2002**, *28*, 53–60.
(18) Takamura, Y.; Narita, S.; Aoki, J.; Uchida, S. Application of High-Pressure Swing Adsorption Process for Improvement of CO_2 Recovery System from Flue Gas. *Can. J. Chem. Eng.* **2001**, *79*, 812–816.
(19) Takamura, Y.; Narita, S.; Aoki, J.; Hironaka, S.; Uchida, S. Evaluation of Dual-Bed Pressure Swing Adsorption for CO_2 Recovery from Boiler Exhaust Gas. *Sep. Purif. Technol.* **2001**, *24*, 519–528.
(20) Tezel, F. H.; Harlick, P.; Sirkecioglu, A. Adsorption of Nitrogen and Carbon Dioxide on ZSM-5. Proceedings of the 12th International Zeolite Conference in Baltimore, MD, July 5−10, 1998.
(21) Tierney, M. J.; Scott, H. S.; Erb, T.; Prasertmanukitch, S. The Purification of Dilute CO_2/Air Solutions with an Annular Bed Adsorber: Numerical and Experimental Investigations. *Sep. Purif. Technol.* **1999**, *17*, 159–171.
(22) Zhang, Z.; Guan, J.; Ye, Z. Separation of a Nitrogen-Carbon Dioxide Mixture by Rapid Pressure Swing Adsorption. *Adsorption* **1998**, *4*, 173–177.
(23) Karger, J.; Ruthven, D. M. *Diffusion in Zeolites and Other Microporous Solids*; John Wiley and Sons Inc.: New York, NY, 1992; pp 467−512.
(24) Lewis, W. K.; Gilliland, E. R.; Chertow, B.; Cadogan, W. P. Absorption Equilibria: Hydrocarbon Gas Mixtures. *Ind. Eng. Chem.* **1951**, *42*, 1319–1326.
(25) Yang, R. T. *Gas Separation by Adsorption Process*; Butterworth Publishers: Stoneham, MA. 1987; pp 9−338.
(26) Van der Vlist, E.; Meijden, J. Van der. Determination of the Adsorption Isotherms of the Components of Binary Gas Mixtures by Gas Chromatography. *J. Chromatogr.* **1973**, *79*, 1–13.
(27) Shah, D. B.; Ruthven, D. M. Measurement of Zeolite Diffusivities by Chromatography. *AIChE J.* **1977**, *23*, 804–810.
(28) Tezel, F. H.; Tezel, H. O.; Ruthven, D. M. Determination of Pure and Binary Isotherms for Nitrogen and Krypton. *J. Colloid Interface Sci.* **1992**, *149*, 197–207.
(29) Heslop, M. J.; Buffman, B. A.; Mason, G. A Test of the Polynomial-Fitting Method of Determining Binary-Gas-Mixture Adsorption Equilibria. *Ind. Eng. Chem. Res.* **1996**, *35*, 1456–1466.
(30) Kabir, H.; Grevillot, G.; Tondeur, D. Equilibria and Activity Coefficients for Non-Ideal Adsorbed Mixtures from Perturbation Chromatography. *Chem. Eng. Sci.* **1998**, *53*, 1639–1654.
(31) Harlick, P. J. E.; Tezel, F. H. A Novel Solution Method for Interpreting Binary Adsorption Isotherms from Concentration Pulse Chromatography Data. *Adsorption* **2000**, *6*, 293–309.
(32) Langmuir, I. The Adsorption of Gazes on Platine Surfaces Glass Mica and Platinum. *J. Am. Chem. Soc.* **1918**, *40*, 1361–1403.
(33) Do, D. D. *Adsorption Analysis: Equilibria and Kinetics*; Imperial College Press: London, UK, 1998; pp 1−148.
(34) Freundlich, H. Of the Adsorption of Gases. Section II. Kinetics and Energetics of Gas Adsorption. Introductory Paper to Section II. *Trans. Faraday Soc.* **1932**, *28*, 195–201.
(35) Sips, R. On the Structure of a Catalyst Surface. *J. Chem. Phys.* **1948**, *16*, 490–495.
(36) Cochran, T. W.; Kabel, R. L.; Danner, R. P. Vacancy Solution Theory of Adsorption Using Flory-Huggins Activity Coefficient Equations. *AIChE J.* **1985**, *31*, 268–277.
(37) Cochran, T. W.; Kabel, R. L.; Danner, R. P. The Vacancy Solution Model of Adsorption - Improvements and Recommendations. *AIChE J.* **1985**, *31*, 2075–2082.
(38) Krishna, R.; Vlugt, T. J. H.; Smit, B. Influence of Isotherm Inflection on Diffusion in Silicalite. *Chem. Eng. Sci.* **1999**, *54*, 1751–1757.
(39) Markham, E. C.; Benton, A. F. The Adsorption of Gas Mixtures by Silica. *J. Am. Chem. Soc.* **1931**, *53*, 497−507.
(40) Bowen, T. C.; Vane, L. M. Ethanol, Acetic Acid, and Water Adsorption from Binary and Ternary Liquid Mixtures on High-Silica Zeolites. *Langmuir* **2006**, *22*, 3721–3727.
(41) Tien, C. *Multicomponent Adsorption Equilibrium and Calculations, in Adsorption Calculations and Modeling*; Butterworth-Heinemann: Newton, MA, 1994; Chapter 4, pp 43−69.
(42) Yang, R. T. *Adsorption: Fundamentals and Applications*; Wiley-Interscience: Hoboken, New Jersey, 2003; pp 18−27.
(43) Li, P.; Tezel, F. H. Adsorption Separation of N_2, O_2, CO_2 and CH_4 Gases by β-Zeolite. *Microporous Mesoporous Mater.* **2007**, *98*, 94–101.
(44) Triebe, R. W.; Tezel, F. H. Adsorption of Nitrogen and Carbon Monoxide on Clinoptilolite: Determination and Prediction of Pure and Binary Isotherms. *Can. J. Chem. Eng.* **1995**, *73*, 717–724.
(45) Calleja, G.; Pau, J.; Calles, J. A. Pure and Multicomponent Adsorption Equilibrium of Carbon Dioxide, Ethylene and Propane on ZSM-5 Zeolites with Different Si/Al Ratios. *J. Chem. Eng. Data* **1998**, *43*, 994–1003.
(46) Sircar, S. Excess Properties and Thermodynamics of Multicomponent Gas Adsorption. *J. Chem. Soc., Faraday Trans.* **1985**, *I 81*, 1527–1540.
(47) Sircar, S. R&D Note: Data Representation for Binary and Multicomponent Gas Adsorption Equilibria. *Adsorption* **1996**, *2*, 327–330.
(48) Sircar, S.; Rao, M. B. Heat of Adsorption of Pure Gas and Multicomponent Gas Mixtures on Microporous Adsorbents. In *Surfaces of Nanoparticles and Porous Materials*; Schwarz, J. A., Contescu, C., Eds.; Marcel Dekker: New York, NY, 1998; Chapter *19*, pp 501−528.
(49) Rao, M. B.; Sircar, S. Thermodynamic Consistency for Binary Gas Adsorption Equilibria. *Langmuir* **1999**, *15*, 7258–7267.
(50) Li, P.; Tezel, F. H. Pure and Binary Adsorption Equilibria of Methane and Carbon Dioxide on Silicalite. *Sep. Sci. Technol.* **2007**, *42*, 3131.
(51) Rees, L. V. C.; Bruckner, P.; Hampson, J. Sorption of N_2, CH_4 and CO_2 in Silicalite-1. *Gas Sep. Purif.* **1991**, *5*, 67.
(52) Dunne, J. A.; Mariwala, R.; Rao, M.; Sircar, S. R.; Gorte, J.; Myers, A. L. Calorimetric Heats of Adsorption and Adsorption Isotherms. 1. O_2, N_2, Ar, CO_2, CH_4, C_2H_6, and SF_6 on Silicalite. *Langmuir* **1996**, *12*, 5888.
(53) Choudhary, V. R.; Mayadevi, S. Adsorption of Methane, Ethane, Ethylene, and Carbon Dioxide on Silicalite-1. *Zeolites.* **1996**, *17*, 501.
(54) Harlick, P. J. E.; Tezel, F. H. Use of Concentration Pulse Chromatography for Determining Binary Isotherms: Comparison with Statistically Determined Binary Isotherms. *Adsorption* **2003**, *9*, 275–286.

Received for review April 5, 2007. Accepted April 3, 2008. Financial support received from the Natural Sciences and Engineering Research Council of Canada (NSERC), the Ontario Graduate Scholarship (OGS) Program, and the Canadian Society for Chemical Engineering (CSChE) is gratefully acknowledged.

JE700183Y